Accepted Manuscript

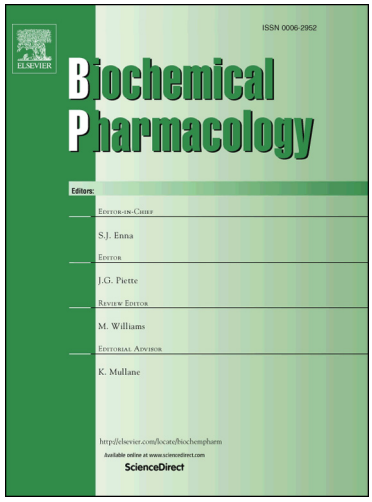

Investigations into the Carbonic Anhydrase Inhibition of COS-Releasing Donor Core Motifs

Andrea K. Steiger, Yu Zhao, Won Jin Choi, Alder Crammond, McKinna R. Tillotson, Michael D. Pluth

PII: S0006-2952(17)30668-8
DOI: https://doi.org/10.1016/j.bcp.2017.11.004
Reference: BCP 12949

To appear in: *Biochemical Pharmacology*

Received Date: 29 September 2017
Accepted Date: 9 November 2017

Please cite this article as: A.K. Steiger, Y. Zhao, W.J. Choi, A. Crammond, M.R. Tillotson, M.D. Pluth, Investigations into the Carbonic Anhydrase Inhibition of COS-Releasing Donor Core Motifs, *Biochemical Pharmacology* (2017), doi: https://doi.org/10.1016/j.bcp.2017.11.004

Investigations into the Carbonic Anhydrase Inhibition of COS-Releasing Donor Core Motifs

Andrea K. Steiger, Yu Zhao, Won Jin Choi, Alder Crammond, McKinna R. Tillotson, Michael D. Pluth*

Department of Chemistry and Biochemistry, Institute of Molecular Biology.

1253 University of Oregon, Eugene, OR 97403, USA.

Email: pluth@uoregon.edu

Phone: (541) 346-7477

Abstract

Carbonyl sulfide (COS) releasing scaffolds are gaining popularity as hydrogen sulfide (H_2S) donors through exploitation of the carbonic anhydrase (CA)-mediated hydrolysis of COS to H_2S. The majority of compounds in this emerging class of donors undergo triggerable decomposition (often referred to as self-immolation) to release COS, and a handful of different COS-releasing structures have been reported. One benefit of this donation strategy is that numerous caged COS-containing core motifs are possible and are poised for development into self-immolative COS/H_2S donors. Because the intermediate release of COS en route to H_2S donation requires CA, it is important that the COS donor motifs do not inhibit CA directly. In this work, we investigate the cytotoxicity and CA inhibition properties of different caged COS donor cores, as well as caged CO_2 and CS_2 motifs and non-self-immolative control compounds. None of the compounds investigated exhibited significant cytotoxicity or enhanced cell proliferation at concentrations up to 100 μM in A549 cells, but we identified four core structures that function as CA inhibitors, thus providing a roadmap for the future development of self-immolative COS/H_2S donor motifs.

Keywords:

Hydrogen sulfide, carbonyl sulfide, carbonic anhydrase

1. Introduction

Hydrogen sulfide (H_2S), now well established as an important gaseous signaling molecule, has been implicated in a wide variety of physiological processes since its initial recognition in 1996.[1-3] H_2S is produced endogenously and maintained at low (mid-nanomolar) concentrations, and the administration of exogenous sulfide has been shown to provide a therapeutic benefit in various applications, including reduction of myocardial infarct size, vasodilation, and decrease in inflammation.[4, 5] For example, GYY4137 and AP39, which undergo slow hydrolysis to release H_2S, have been shown to exhibit anti-inflammatory activity.[6, 7] Additionally, appending H_2S donor scaffolds to non-steroidal anti-inflammatory drugs (NSAIDs) has been used to generate a number of H_2S-NSAID hybrids including ATB-346 and NBS-1120, which are based on naproxen and aspirin derivatives, respectively (Figure 1).[8, 9] Aligned with these positive impacts, new H_2S donation strategies are emerging rapidly, and a number of H_2S-releasing compounds are currently in clinical trials.[10, 11] Recent goals in improving upon H_2S-based therapeutics have included triggerable donation in response to specific (and variable) stimuli, controllable rates of H_2S release, and the ability to append the H_2S-releasing moiety to a variety of scaffolds to potentially access H_2S-drug hybrids.

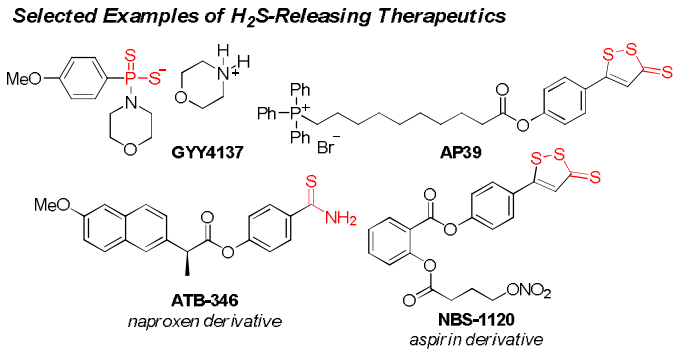

Building from these needs, our lab recently introduced a new strategy for H_2S donation

by using the triggered decomposition (often referred to as self-immolation) of carbonyl sulfide (COS)-releasing motifs (Figure 2a), which leverages the rapid hydrolysis of COS to H_2S by carbonic anhydrase (CA), a ubiquitous mammalian zinc metalloenzyme that normally catalyzes the hydrolysis of CO_2 under near diffusion-limited rates to regulate blood pH levels and tissue CO_2 transport.[12, 13] Since our initial report,[14] a number of related COS-donating scaffolds have been reported for H_2S release.[15-21] Complementing slow-release COS donors,[16] a common strategy has been to engineer self-immolative COS release, which can be activated by different stimuli, including ROS,[21] esterase,[15, 18] light,[17, 20] and bio-orthogonal triggers[19] (selected triggered examples are shown in Figure 2b). Moreover, we recently reported on the kinetics of COS release from several different caged carbonyl sulfide isomers and found that COS/H_2S release profiles can be tuned by structural and isomeric modifications.[22] This work expanded our growing knowledge of potential COS donor scaffolds and provides a resource for researchers wishing to develop COS donor scaffolds to fit a specific need. In addition to providing functional H_2S donor platforms, the availability of such COS donors may allow for the investigation of COS chemical biology, which has been largely under-studied.[23] Critical to using these donor scaffolds for COS investigations or for therapeutic H_2S delivery is the general biocompatibility of the core motifs, including potential direct interactions with CA. The efficient conversion of COS to H_2S in all of the above scaffolds requires CA, so it is imperative to not only understand the mechanism of CA activity in COS hydrolysis, but also to determine whether any of the COS-donating motifs are functional CA inhibitors. Significant prior research has focused on identifying CA inhibitors for therapeutic uses, such as treatment of glaucoma, epilepsy, and mountain sickness, and is the topic of numerous recent reviews.[13, 24, 25] Because the structural scope of active CA inhibitors is

broad and includes many sulfur-containing molecules, including dithiocarbamates and trithiocarbonates,[26, 27] we wanted to determine whether the sulfur-containing cores of possible COS-releasing scaffolds (Figure 2c) exhibit CA inhibition. If a COS-releasing motif functions as a viable CA inhibitor, donor scaffolds built from such motifs are unlikely to find widespread utility as functional H_2S donors. Such investigations are important in understanding the scope of potential COS-releasing structural motifs due to the necessity of CA activity for efficient H_2S release from COS donors

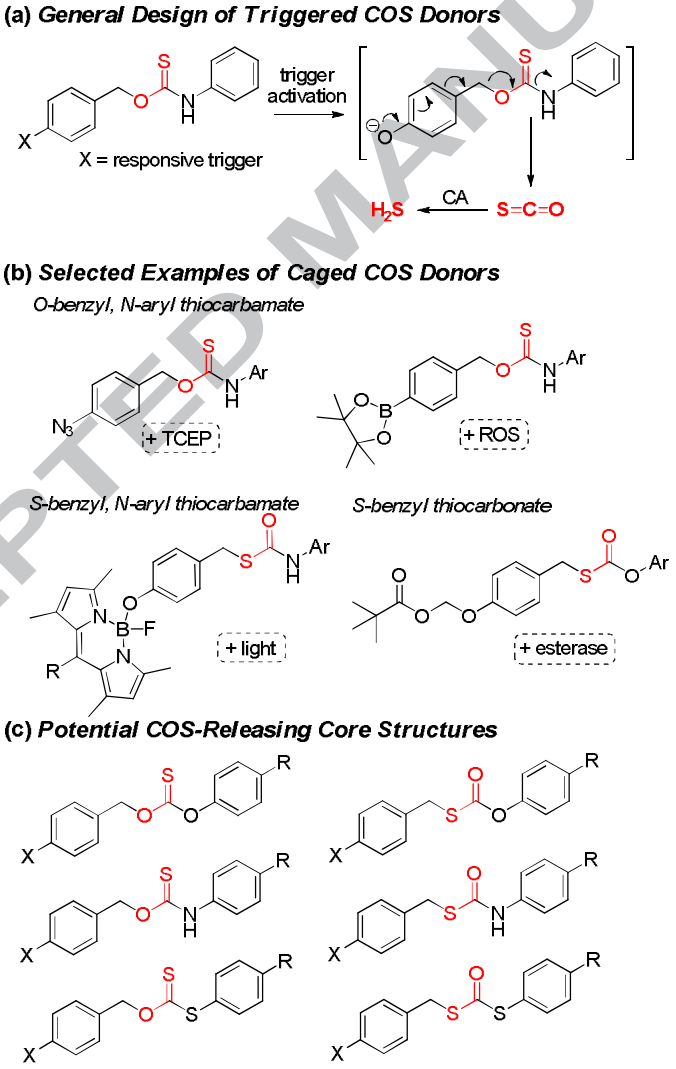

2. Materials and Methods

2.1 Synthetic Materials

Reagents were purchased from Sigma-Aldrich (St. Louis, MO), Alfa-Aesar (Haverhill, MA), or Tokyo Chemical Industry (TCI, Portland, OR) and used as received. Compounds **1**-**15** were synthesized as previously reported. Spectroscopic grade, inhibitor-free THF and DCM were deoxygenated by sparging with argon followed by passage through a Pure Process Technologies solvent purification system to remove water. Deuterated solvents were purchased from Cambridge Isotope Laboratories (Tewksbury, MA) and used as received. Silica gel (SiliaFlash F60, Silicycle, 230-400 mesh) was used for column chromatography. ^{1}H, and ^{13}C{^{1}H} NMR spectra were recorded on a Bruker 500 MHz instrument. Chemical shifts are reported in ppm relative to residual protic solvent resonances.

2.2 *Spectroscopic Materials*

Tris-HCl buffer was prepared from Tris hydrochloride (Sigma Aldrich, 50 mM) and deionized water obtained from a Synergy UV Millipore Water System and adjusted to pH 8.5 with a SevenMulti pH Probe (Mettler Toledo). UV-visible spectra were acquired on a Cary 60 UV-vis spectrometer equipped with a Quantum Northwest TC-1 temperature controller.

2.3 *Cell Culture Materials*

A549 cells obtained from ATCC (Manassas, VA) were grown in a 5% CO_2 incubator at 37 °C in Dulbecco's Modified Eagle Medium (Gibco (Dublin, Ireland), high glucose, phenol red) with

10% FBS (VWR, Radnor, PA) and 1% penicillin streptomycin (Gibco). Cells were passaged (up to p 25) every 1-3 days upon reaching 85-90% confluency. Absorbance measurements were acquired using a Tecan Safire2 microplate reader.

2.4 *Synthesis*

2.4.1 *General synthetic procedure A (Figure 3a)*

The alcohol, thiol, or amine starting material (1.0 equiv.) was combined with phenyl isothiocyanate or phenyl isocyanate (1.0 equiv.) in anhydrous THF (15 mL) at 0 °C, followed by the addition of base (1.2 equiv.). The resultant mixture was stirred at 0 °C for 20 min, after which the ice bath was removed, and the reaction mixture was stirred at r.t. until the completion of the reaction as indicated by TLC. The reaction was quenched by adding brine (30 mL), and the aqueous solution was extracted with ethyl acetate (3 × 15 mL). The organic layers were combined, dried over $MgSO_4$, and evaporated under vacuum. The crude products from each reaction were purified by column chromatography.

Compound **1** was prepared from benzyl alcohol and phenyl isothiocyanate in the presence of NaH (yield: 75%). Compound **2** was prepared from benzyl mercaptan and phenyl isocyanate in the presence of NaH (yield: 38%). Compound **6** was prepared from benzyl alcohol and phenyl isocyanate in the presence of TEA (yield: 20%). Compound **9** was prepared from benzyl mercaptan and phenyl isothiocyanate in the presence of NaH (yield: 75%). Compound **14** was prepared from benzyl amine and phenyl isocyanate in the presence of TEA (yield: 88%). Compound **15** was prepared from benzyl amine and phenyl isothiocyanate in the presence of TEA. (yield: 64%). Characterization data for previously-reported compounds **1**, **2**, **6**, **9**, **14**, and **15** match the reported data. [21, 28-32]

2.4.2 *General synthetic procedure B (Figure 3b)*

The alcohol, thiol, or amine starting material (1.0 equiv.) was combined with the phenyl chloroformate reagent (1.0 equiv.) in anhydrous DCM (15 mL) at 0 °C, followed by the addition of base (1.0 equiv.). The resultant solution was stirred at 0 °C for 20 min, after which the ice bath was removed, and the reaction mixture was stirred at r.t. until the completion of the reaction as indicated by TLC. The reaction was quenched by adding brine (30 mL), and the aqueous solution was extracted with ethyl acetate (3 × 15 mL). The organic layers were combined, dried over $MgSO_4$, and evaporated under vacuum. The crude products from each reaction were purified by column chromatography.

Compound **3** was prepared from benzyl alcohol and phenyl chlorothionoformate in the presence of pyridine (yield: 57%). ^{1}H NMR (500 MHz, $CDCl_3$) δ (ppm): 7.55 (m, 7H), 7.33 (t, J = 10.0 Hz, 1H), 7.16 (d, J = 10.0 Hz, 2H), 5.60 (s, 2H). ^{13}C{^{1}H} NMR (125 MHz, $CDCl_3$) δ (ppm): 195.0, 153.5, 134.2, 129.6, 128.8, 128.7, 128.6, 126.6, 122.0, 75.6. Compound **4** was prepared from benzyl mercaptan and phenyl chloroformate in the presence of TEA (yield: 73%). The characterization data match the reported data.[32] Compound **5** was prepared from benzyl mercaptan and phenyl thiochloroformate in the presence of TEA (yield: 71%). ^{1}H NMR (500 MHz, DMSO-d_6) δ (ppm): 7.53 (m, 5H), 7.32 (m, 4H), 7.27 (m, 1H), 4.25 (s, 2H). ^{13}C{^{1}H} NMR (125 MHz, DMSO-d_6) δ (ppm): 188.6, 137.3, 135.8, 131.1, 130.2, 129.4, 129.1, 127.9, 126.5, 34.9. Compound **7** was prepared from benzyl alcohol and phenyl chloroformate in the presence of TEA (yield: 62%). The characterization data match the reported data.[28] Compound **8** was prepared from benzyl alcohol and phenyl thiochloroformate in the presence of NaH (yield: 32%). ^{1}H NMR (500 MHz, CDCl3) δ (ppm): 7.57 (m, 2H), 7.44 (m, 3H), 7.39 (m, 5H), 5.29 (s,

2H). $^{13}C\{^{1}H\}$ NMR (125 MHz, $CDCl_3$) δ (ppm): 167.9,135.0, 134.9, 129.6, 129.2, 128.6, 128.5, 127.7, 69.4. Compound **10** was prepared from benzyl mercaptan and phenyl chlorothionoformate in the presence of pyridine (yield: 43%). The characterization data match the reported data.[33] Compound **11** was prepared from benzyl amine and phenyl chloroformate in the presence of TEA (yield: 82%). The characterization data match the reported data.[34] Compound **12** was prepared from benzyl amine and phenyl thiochloroformate in the presence of pyridine (yield: 57%). ^{1}H NMR (500 MHz, DMSO-d_6) δ (ppm): 8.85 (s, 1H), 7.46 (m, 2H), 7.41 (s, 3H), 7.35 (t, J = 5.0 Hz, 2H), 7.26 (d, J = 10.0 Hz, 3H), 4.32 (s, 2H). $^{13}C\{^{1}H\}$ NMR (125 MHz, DMSO-d_6) δ (ppm): 164.6, 139.3, 135.4, 129.4, 129.3, 129.1, 128.8, 127.8, 127.5, 44.7. Compound **13** was prepared from benzyl amine and phenyl chlorodithioformate in the presence of TEA (yield: 49%). ^{1}H NMR (500 MHz, $CDCl_3$) δ (ppm): 7.61 (m, 2H), 7.50 (m, 3H), 7.32 (m, 3H), 7.17 (d, J = 10.0 Hz, 2H), 6.86 (br, 1H), 4.86 (d, J = 5.0 Hz, 2H). $^{13}C\{^{1}H\}$ NMR (125 MHz, $CDCl_3$) δ (ppm): 195.3, 135.8, 135.6, 131.2, 130.4, 128.9, 128.6, 128.0, 127.5, 50.2.

2.5 Cytotoxicity Assays

Stock solutions of the compounds (20 mM, 10 mM, 5 mM, 2 mM) were prepared in DMSO via serial dilution and used to make 100 µM, 50 µM, 25 µM, and 10 µM solutions of each compound in DMEM (no phenol red, no FBS). 96-Well plates were seeded with ~20,000 cells/well overnight prior to cytotoxicity experiments. Cells were washed with PBS (Gibco) and incubated with the desired compound or with vehicle (0.5% DMSO) for one hour prior to being washed with PBS and incubated with CCK-8 solution (10% in DMEM). After 1 hour, the absorbance at 450 nm was measured on a plate reader, and the cell survival was calculated as a percent of the control and normalized to the vehicle group. The results are expressed as mean ±

SD (n = 6).

2.6 Determination of CA Inhibition

Stock solutions of each compound (20 mM in DMSO), acetazolamide (20 mM in DMSO), *p*-nitrophenylacetate *(*pNPA, 15 mM in ethanol), and CA (7.5 mg/mL in Tris buffer) were prepared and stored at 2-4 °C until immediately prior to use. pNPA (20 µL) was injected into the Tris HCl buffer (3 mL) immediately followed by the desired compound of interest (7.5 µL) with stirring at 37.00 ± 0.05 °C. Data collection began immediately prior to injection of CA (20 µL) and continued until the production of pNP was complete, as determined by a plateau in absorbance at 405 nm. Absorption data was fit to a first-order exponential equation in Origin 8 to obtain pseudo first-order rate data, which are reported in units of s^{-1}. All trials were completed in triplicate and rates are reported as mean ± SD (n = 3).

3. Results

3.1 *Synthesis of Model Compounds*

The 15 model compounds used in our investigations were prepared using two general procedures. In synthetic procedure A (Figure 3a), one equivalent of an alcohol, thiol, or amine was combined with one equivalent of phenyl isothiocyanate or phenyl isocyanate and base and was stirred until completion of the reaction. Following an extraction and purification by column chromatography, compounds **1**, **2**, **6**, **9**, and **14-15** were isolated in 20-88% yield. In synthetic procedure B (Figure 3b), one equivalent of the alcohol, thiol, or amine starting material was combined with one equivalent of phenyl chloroformate and base. When the reaction was complete, the product was washed, extracted, and purified by column chromatography. Compounds **3-5**, **7-8**, and **10-13** were isolated in 32-82% yield.

Our initial report of caged COS release utilized an *O*-alkyl thiocarbamate scaffold, but *S*-alkyl thiocarbamates and thiocarbonates have also been reported.[15, 17, 22] Depending on the placement of the COS moiety in the caged core, there are different constitutional isomers that can release COS, which motivated our selection of model compounds **1-5** (Figure 3c). Similarly, the availability of caged CO_2 compounds, which generate CO_2/H_2O rather than COS/H_2S, prompted our investigation of control compounds **6-8** (Figure 3d). Additionally, the recent interest in CS_2 donor development prompted our inclusion of dithiocarbamates **9-10** (Figure 3e).[35] Finally, we included isomers **11-15** as control compounds, which have similar functional motifs but lack the caged COS core (Figure 3f). For each of these model compounds, our goal was to determine whether the core structures exerted cytotoxicity or cell proliferative effects and also to measure the CA inhibition profiles for each compound to better guide future COS donor development.

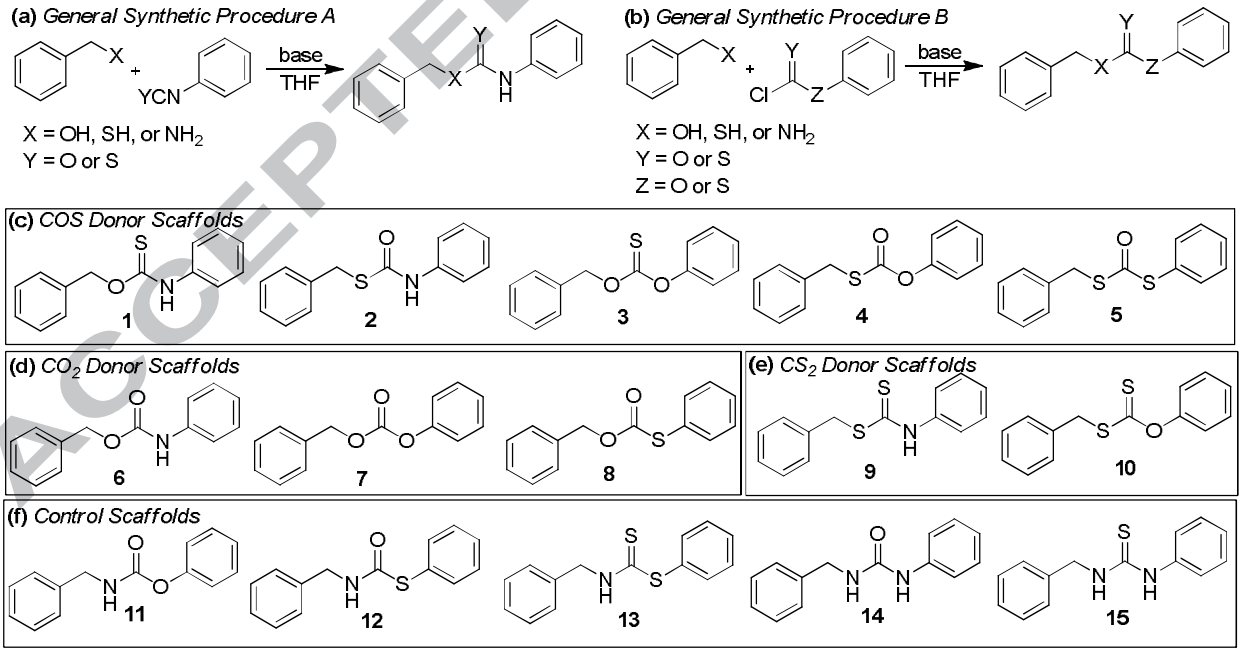

3.2 *Cytotoxicity Evaluation*

Prior to measuring CA inhibition profiles, we first measured the cytotoxicity of each compound in A549 human lung adenocarcinoma cells using the CCK-8 cell proliferation assay. We chose concentrations ranging from 10 – 100 μM for each compound, which corresponds to the general concentration ranges typically used in biological experiments that use H_2S-donating compounds. Incubation of A549 with 10, 25, 50, or 100 μM of each compound did not result in significant cytotoxicity or proliferation, suggesting that the inherent core structures from each model compound do not significantly impact cell viability (Figure 4).

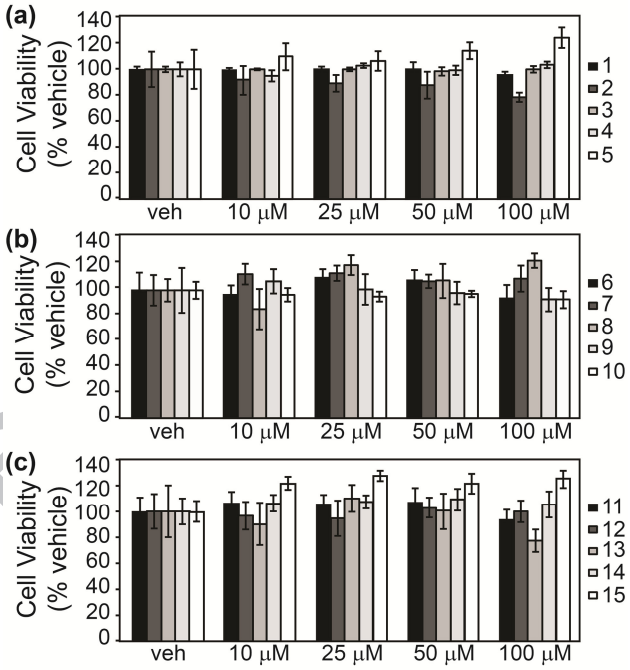

3.3 *Determination of CA Inhibitors*

To investigate the potential CA inhibition properties of each of the selected scaffolds, we used CA-mediated *p*-nitrophenyl acetate (pNPA) hydrolysis as a model system for measuring CA activity / inhibition. The CA-mediated hydrolysis of pNPA is slower than the near diffusion-

limited hydrolysis of CO_2, and the *p*-nitrophenol (pNP) product has a characteristic absorbance at 405 nM, thus providing a simple method to measure CA activities by UV-vis spectroscopy (Figure 5a)[36]. For each compound, we measured the rate of pNPA hydrolysis to pNP and compared these observed rates to those of CA alone, as well as the rate in the presence of the common CA inhibitor acetazolamide (AAA, Figure 5b). In each case, the rate of production of pNP was then fit directly to a first-order exponential equation. Of the 15 compounds tested, 11 failed to produce significant changes in the rate of pNPA hydrolysis, suggesting that these compounds do not exhibit significant CA inhibition at concentrations typically used in H_2S donor experiments. Four compounds, however, were found to inhibit CA activity: **2**, **9**, **12**, and **13**. Of these compounds, **2** and **9** were moderate inhibitors and decreased the rate of pNPA hydrolysis by about 50%. By comparison, compounds **12** and **13** were much more effective CA inhibitors and decreased the rate of hydrolysis to approximately that seen in the presence of AAA, which is recognized as a strong CA inhibitor (Figure 5c-f).

-

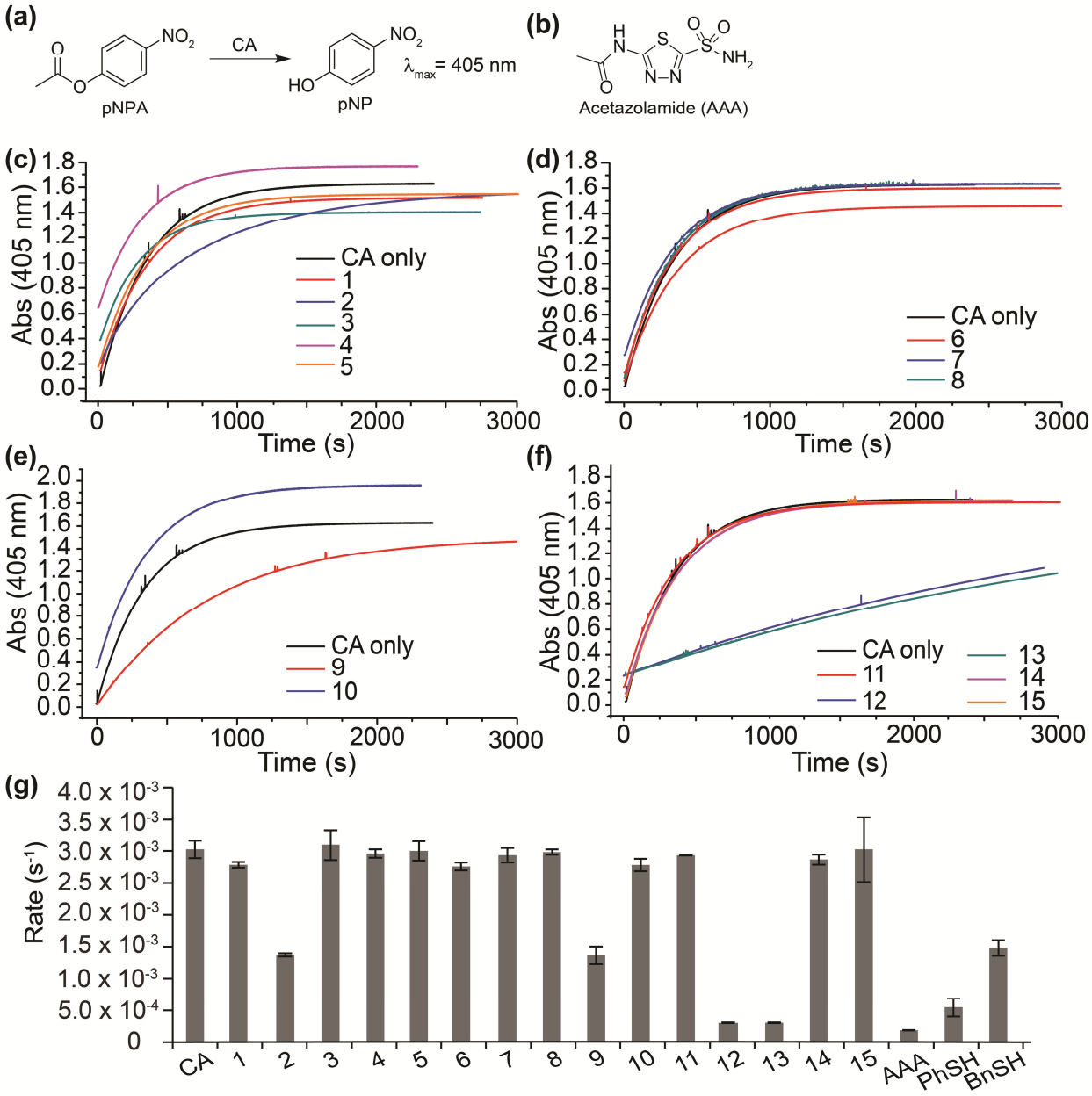

3.4 *Inhibition studies with potential decomposition products*

In addition to the 15 compounds examined above, we also investigated the CA inhibition properties of thiophenol and benzyl thiol because these thiols could potentially be generated as hydrolysis and/or decomposition products of **2**, **9**, **12**, and **13**. (vide infra). We found both thiophenol and benzyl thiol to inhibit CA (Figure 5g). The rate of hydrolysis in the presence of

thiophenol alone was found to be similar to that of **12** and **13**, both of which, if deprotonated, would decompose to thiophenol. Similarly, the rate of pNPA hydrolysis observed in the presence of benzyl thiol is similar to that of **2** and **9**, which would decompose to benzyl thiol.

4. Discussion

The recent introduction and adoption of triggered COS-releasing compounds for H_2S donation highlights the potential of this strategy to access a broad class of H_2S donors with potential therapeutic properties. In addition to providing functional COS/H_2S donor platforms, the use of analogous CO_2/H_2O-releasing compounds provide key control compounds that undergo the same self-immolative chemistry to generate the same organic byproducts as the canonical donors, but which do not release COS/H_2S. For all such scaffolds, a key component of the COS/H_2S donor strategy is the requirement of CA-mediated COS hydrolysis to H_2S. Because of this requirement, the donor motifs should not interfere with CA activity. With these considerations in mind, we wanted to measure cytotoxicity profiles and CA inhibition data for these potential COS-releasing moieties to help determine the most promising scaffolds for caged COS release.

We identified a library of 15 compounds that include known and potential caged COS scaffolds, caged CO_2 and CS_2 motifs, and related control compounds as described in the Results section. Although each of these compounds represents a scaffold that could be used in a donor or control compound, they do not contain triggering moieties to allow for decomposition, meaning that they should not release COS spontaneously. By investigating the cytotoxicity and CA inhibition profile of each core motif, we hoped to identify the core structures that do not affect CA activity for future COS/H_2S donor design.

As outlined in the Results section, none of the prepared model compounds were found to be cytotoxic in A549 cells at concentrations below 100 μM, suggesting that the core motifs are not inherently cytotoxic at concentration ranges typically used in H_2S donation studies. Of the 15 compounds investigated, however, we did identify four compounds that inhibit CA activity: **2**, **9**, **12**, and **13** (Figure 6a). At first, the only similarity between these compounds appeared to be the presence of a sulfur atom adjacent to the thiocarbonyl moiety. We also noticed, however, that deprotonation of the amide NH in these compounds could lead to decomposition to form a thiol-containing byproduct (benzyl thiol for **2** and **9** or thiophenol for **12** and **13**, Figure 6b). We hypothesized that these thiol byproducts may be responsible for the observed inhibitory properties, rather than the thiocarbamate/dithiocarbamate scaffolds directly. Further supporting this hypothesis, we measured the inhibitory effects of benzyl thiol and thiophenol. Benzyl thiol exhibited similar CA inhibitory profiles to **2** and **9**, and thiophenol inhibited CA similarly to **12** and **13**. Aside from the shown CA inhibition properties, this additionally suggests the instability of these scaffolds at even moderately basic conditions, making them less reliable as COS donor constructs or as suitable controls.

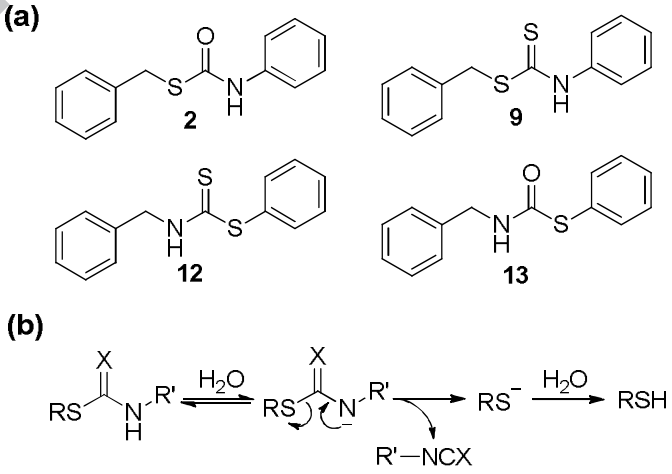

In combination with recent work investigating stability and rate of COS/H_2S release from

different COS-releasing scaffolds,[22] the present work provides an important resource for selecting the best scaffolds for COS donation in the design of H_2S therapeutics. Four scaffolds (**1**, **3**, **4**, and **5**) were identified that have either been reported to release COS or are likely to release COS through self-immolation that do not inhibit CA. These motifs are likely ideal starting points in the design of new COS/H_2S donor motifs. Although this work provides the first insights into the potential CA inhibition properties of COS/H_2S donor scaffolds, any structural modifications could impact the extent of inhibition, which will likely require future constructs to be tested for CA inhibition directly. Additionally, the identification of thiocarbamate **2** as a CA inhibitor should not completely eliminate this *S*-alkyl thiocarbamate motif from consideration as a COS/H_2S donor core, because further functionalization of the core structure may impact or reduce the CA inhibition profiles. Indeed, similar scaffolds have been shown to be successful COS donors in recent reports.[15, 17] Future work is required to determine the precise consequences of using a COS donor that inhibits CA as an H_2S donor, but the efficiency, rate of decomposition, and rate of H_2S production may all be affected. Through the rational selection of COS donor cores that provide efficacious COS/H_2S release rates, suitable stability in the presence of biological milieu, and minimal CA inhibition, we expect the field of COS/H_2S donors will continue to expand rapidly and provide access to new motifs with pharmacologically-relevant activities.

Conflict of Interest

The authors declare no conflict of interest.

Acknowledgements

Research reported in this publication was supported in part by the Sloan Foundation, Dreyfus Foundation, the NIH (MDP; R01GM113030), and the NSF/GRFP (AKS; DGE-1309047). NMR infrastructure at the UO is supported by the NSF (CHE-1427987).

References

[1] K. Abe, H. Kimura, The possible role of hydrogen sulfide as an endogenous neuromodulator, Journal of Neuroscience 16(3) (1996) 1066-1071.

[2] H. Kimura, N. Shibuya, Y. Kimura, Hydrogen sulfide is a signaling molecule and a cytoprotectant, Antioxid Redox Signal 17(1) (2012) 45-57.

[3] R. Wang, Two's company, three's a crowd: can H2S be the third endogenous gaseous transmitter?, FASEB J 16(13) (2002) 1792-8.

[4] R. Wang, Physiological implications of hydrogen sulfide: a whiff exploration that blossomed, Physiol Rev 92(2) (2012) 791-896.

[5] K.R. Olson, The therapeutic potential of hydrogen sulfide: separating hype from hope, Am J Physiol Regul Integr Comp Physiol 301(2) (2011) R297-312.

[6] L. Li, M. Whiteman, Y.Y. Guan, K.L. Neo, Y. Cheng, S.W. Lee, Y. Zhao, R. Baskar, C.H. Tan, P.K. Moore, Characterization of a novel, water-soluble hydrogen sulfide-releasing molecule (GYY4137): new insights into the biology of hydrogen sulfide, Circulation 117(18) (2008) 2351-60.

[7] B. Szczesny, K. Modis, K. Yanagi, C. Coletta, S. Le Trionnaire, A. Perry, M.E. Wood, M. Whiteman, C. Szabo, AP39, a novel mitochondria-targeted hydrogen sulfide donor, stimulates cellular bioenergetics, exerts cytoprotective effects and protects against the loss of mitochondrial DNA integrity in oxidatively stressed endothelial cells in vitro, Nitric Oxide 41 (2014) 120-30.

[8] R. Kodela, M. Chattopadhyay, K. Kashfi, NOSH-Aspirin: A Novel Nitric Oxide-Hydrogen Sulfide-Releasing Hybrid: A New Class of Anti-inflammatory Pharmaceuticals, ACS Med Chem Lett 3(3) (2012) 257-262.

[9] J.L. Wallace, G. Caliendo, V. Santagada, G. Cirino, Markedly reduced toxicity of a hydrogen sulphide-releasing derivative of naproxen (ATB-346), Br J Pharmacol 159(6) (2010) 1236-46.

[10] J.L. Wallace, R. Wang, Hydrogen sulfide-based therapeutics: exploiting a unique but ubiquitous gasotransmitter, Nat Rev Drug Discov 14(5) (2015) 329-45.

[11] Y. Zheng, B. Yu, L.K. De La Cruz, M. Roy Choudhury, A. Anifowose, B. Wang, Toward Hydrogen Sulfide Based Therapeutics: Critical Drug Delivery and Developability Issues, Med Res Rev (2017) DOI: 10.1002/med.21433.

[12] C.P. Chengelis, R.A. Neal, Studies of carbonyl sulfide toxicity: Metabolism by carbonic anhydrase, Toxicology and Applied Pharmacology 55(1) (1980) 198-202.

[13] T.H. Maren, Carbonic anhydrase: chemistry, physiology, and inhibition, Physiol Rev 47(4) (1967) 595-781.

[14] A.K. Steiger, S. Pardue, C.G. Kevil, M.D. Pluth, Self-Immolative Thiocarbamates Provide Access to Triggered H2S Donors and Analyte Replacement Fluorescent Probes, J Am Chem Soc 138(23) (2016) 7256-9.

[15] P. Chauhan, P. Bora, G. Ravikumar, S. Jos, H. Chakrapani, Esterase Activated Carbonyl Sulfide/Hydrogen Sulfide (H2S) Donors, Org Lett 19(1) (2017) 62-65.

[16] C.R. Powell, J.C. Foster, B. Okyere, M.H. Theus, J.B. Matson, Therapeutic Delivery of H2S via COS: Small Molecule and Polymeric Donors with Benign Byproducts, J Am Chem Soc 138(41) (2016) 13477-13480.

[17] A.K. Sharma, M. Nair, P. Chauhan, K. Gupta, D.K. Saini, H. Chakrapani, Visible-Light-Triggered Uncaging of Carbonyl Sulfide for Hydrogen Sulfide (H2S) Release, Org Lett 19(18) (2017) 4822-4825.

[18] A.K. Steiger, M. Marcatti, C. Szabo, B. Szczesny, M.D. Pluth, Inhibition of Mitochondrial Bioenergetics by Esterase-Triggered COS/H2S Donors, ACS Chem Biol 12(8) (2017) 2117-2123.

[19] A.K. Steiger, Y. Yang, M. Royzen, M.D. Pluth, Bio-orthogonal "click-and-release" donation of caged carbonyl sulfide (COS) and hydrogen sulfide (H2S), Chem Commun (Camb) 53(8) (2017) 1378-1380.

[20] Y. Zhao, S.G. Bolton, M.D. Pluth, Light-Activated COS/H2S Donation from Photocaged Thiocarbamates, Org Lett 19(9) (2017) 2278-2281.

[21] Y. Zhao, M.D. Pluth, Hydrogen Sulfide Donors Activated by Reactive Oxygen Species, Angew Chem Int Ed Engl 55(47) (2016) 14638-14642.

[22] Y. Zhao, H.A. Henthorn, M.D. Pluth, Kinetic Insights into Hydrogen Sulfide Delivery from Caged-Carbonyl Sulfide Isomeric Donor Platforms, J Am Chem Soc (2017) DOI: 10.1021/jacs.7b09527.

[23] A.K. Steiger, Y. Zhao, M.D. Pluth, Emerging Roles of Carbonyl Sulfide in Chemical Biology: Sulfide Transporter or Gasotransmitter?, Antioxid Redox Signal (2017) DOI: 10.1089/ars.2017.7119.

[24] C.T. Supuran, Carbonic anhydrase inhibitors, Bioorg Med Chem Lett 20(12) (2010) 3467-74.

[25] C.T. Supuran, A. Scozzafava, A. Casini, Carbonic anhydrase inhibitors, Med Res Rev 23(2) (2003) 146-89.

[26] F. Carta, M. Aggarwal, A. Maresca, A. Scozzafava, R. McKenna, E. Masini, C.T. Supuran, Dithiocarbamates strongly inhibit carbonic anhydrases and show antiglaucoma action in vivo, J Med Chem 55(4) (2012) 1721-30.

[27] F. Carta, A. Akdemir, A. Scozzafava, E. Masini, C.T. Supuran, Xanthates and trithiocarbonates strongly inhibit carbonic anhydrases and show antiglaucoma effects in vivo, J Med Chem 56(11) (2013) 4691-700.

[28] J.B. Christensen, M. Pittelkow, R. Lewinsky, Selective Synthesis of Carbamate Protected Polyamines Using Alkyl Phenyl Carbonates, Synthesis (15) (2002) 2195-2202.

[29] M. Hatano, S. Kamiya, K. Moriyama, K. Ishihara, Lanthanum(III) isopropoxide catalyzed chemoselective transesterification of dimethyl carbonate and methyl carbamates, Org Lett 13(3) (2011) 430-3.

[30] K. Inamoto, C. Hasegawa, K. Hiroya, T. Doi, Palladium-catalyzed synthesis of 2-substituted benzothiazoles via a C-H functionalization/intramolecular C-S bond formation process, Org Lett 10(22) (2008) 5147-50.

[31] S. Lu, X. Zhang, A Novel One-Pot Solvent-Free, Triethylamine-Assisted, Selenium-Catalyzed Synthesis of Thiocarbamates from Nitroarenes, Carbon Monoxide, and Thiols, Synlett 2005(10) (2005) 1535-1538.

[32] B. Movassagh, M. Tavoosi, Synthesis of S-Aryl/Alkyl Thiolcarbonates from Disulfides and Chloroformates in the Presence of the Zn/AlCl3 System, Monatshefte für Chemie - Chemical Monthly 139(3) (2008) 251-253.

[33] R.T.A.M. John Chiefari, Catherine L. Moad, Graeme Moad, Ezio Rizzardo, Almar Postma, Melissa A. Skidmore, San H. Thang, Thiocarbonylthio Compounds (SC(Z)S−R) in Free Radical Polymerization with Reversible Addition-Fragmentation Chain Transfer (RAFT Polymerization). Effect of the Activating Group Z, Macromolecules 36(7) (2003) 2273-2283.

[34] M.D. Stephens, N. Yodsanit, C. Melander, Evaluation of ethyl N-(2-phenethyl) carbamate analogues as biofilm inhibitors of methicillin resistant Staphylococcus aureus, Org Biomol Chem 14(28) (2016) 6853-6.

[35] A.W. DeMartino, M.L. Souza, P.C. Ford, Uncaging carbon disulfide. Delivery platforms for potential pharmacological applications: a mechanistic approach, Chem. Sci. 8(10) (2017) 7186-7196.

[36] Y. Pocker, J.T. Stone, The Catalytic Versatility of Erythrocyte Carbonic Anhydrase. III. Kinetic Studies of the Enzyme-Catalyzed Hydrolysis of p-Nitrophenyl Acetate*, Biochemistry 6(3) (1967) 668-678.

Figure 1. Selected examples of H_2S-releasing therapeutics currently in various stages of clinical development.

Figure 2. (a) General strategy for H_2S generation from COS-releasing molecules. A caged thiocarbamate is shown as an example system. (b) Selected examples of triggered COS donors with different core structural motifs. (c) Potential thiocarbonate, thiocarbamate, and dithiocarbonate motifs that could function as COS/H_2S donors.

Figure 3: (a), (b) General synthetic procedures to prepare model compounds. Structures of the model compounds prepared and investigated in this study include (c) COS donor scaffolds (**1**-**5**), (d) CO_2 donor scaffolds (**6**-**8**), (e) CS_2 donor scaffolds (**9**-**10**), and (f) control scaffolds (**11**-**15**).

Figure 4. CCK-8 cytotoxicity assay of compounds 1-15. The cytotoxicity of each compound was investigated in A549 cells at 10, 25, 50 and 100 μM using the CCK-8 cell counting assay and compared to the DMSO vehicle. (a) caged COS scaffolds (**1-5**), (b) caged CO_2 (**6**-**8**) and CS_2 (**9**-**10**) scaffolds, and (c) control scaffolds (**11-15**).

Figure 5. (a) CA-mediated hydrolysis of pNPA to form pNP. (b) Strucutre of known CA inhibitor AAA. pNPA assay of (c) caged COS scaffolds, (d) caged CO_2 scaffolds, (e) caged CS_2 scaffolds, and (f) control scaffolds. (g) Absorbance data was fit to a first order exponential to determine rate of hydrolysis in the presence of each compound and compared to AAA, PhSH, and BnSH.

Figure 6. (a) Structures of compounds identified as CA inhibitors. (b) Mechanism for production of thiophenol or benzyl thiol following deprotonation of **2**, **9**, **12**, or **13**.